2004

Melt flow control using magnetic fields and magnetic field gradients

Nicholas Zabaras, *Cornell University*
Baskar Ganapathysubramanian, *Cornell University*

COMPUTATIONAL MECHANICS
WCCM VI in conjunction with APCOM'04, *Sept. 5-10, 2004, Beijing, China*

Melt flow control using magnetic fields and magnetic field gradients

N. Zabaras[1*], B. Ganapathysubramanian[2]

[1,2] *Materials Process Design and Control Laboratory, Sibley School of Mechanical and Aerospace Engineering, Cornell University, 188 Frank H.T. Rhodes Hall, Ithaca, NY, 14853-3801, USA.*
e-mail: zabaras@cornell.edu, bg74@cornell.edu

Abstract Solidification of materials to near net shape is one of the most commonly used and economical methods of manufacturing. Different industries impose different restrictions on the solidification process. For example, single crystal growth requires a planar growth front, whereas casting requires homogenous material distribution. There are various techniques to control the flow in the melt to achieve the required objectives. Magnetic field based control techniques have become the most popular, commercially used methods. The application of a non-uniform external magnetic field produces an extra body force (Kelvin force) in the melt which along with the Lorenz force can be used to effectively control solidification and crystal growth processes. The physics behind the application of a time varying magnetic gradient on the flow is discussed and a coupled set of equations governing the fluid flow, thermal and concentration fields is determined. In this work, we only consider the solidification of non-conducting melts in the presence of magnetic fields and magnetic field gradients. A computational method for the design of solidification of non-conducting materials is developed such that a prescribed characteristic during solidification is achieved. An appropriate cost functional is defined. The cost function is here taken as the square of the L_2 norm of the deviation of the velocity field in the melt region from conditions corresponding to convection-less growth. The adjoint method for the inverse design of continuum processes is adopted in this framework. A continuum adjoint system is derived to calculate the adjoint temperature, concentration and velocity such that the gradient of the cost functional can be expressed analytically. The cost functional is minimized using the conjugate gradient method with a finite element realization of the continuum direct, sensitivity and adjoint problems. An example of designing the time history of the magnetic field is presented. Similar developments to the ones discussed here have been achieved for the solidification of conducting melts. Thus the developed methodology has wide applications in crystal growth and the directional solidification of materials, organic compounds and biological macromolecules.

Key words: inverse design, solidification, magnetic fields, magnetic field gradients, magneto-hydrodynamics, adjoint formulation

INTRODUCTION

Various design and control problems of interest can often be posed as inverse problems in which, in addition to the various field equations, incomplete conditions are given on one part of the boundary, whereas over-specified boundary conditions are available on another part of the boundary or inside the domain (Tichonov [1]). In the context of thermal design, inverse heat conduction problems have been well studied due to their widespread engineering applications as well as their simplicity. Research attention has also been directed towards inverse convection and fluid flow control problems due to their practical relevance (Gunzberger et al. [2]). These methodologies have simultaneously been extended to solidification process design by Zabaras and colleagues [3]-[4]. The main emphasis of these papers

has been the design of mold heating/cooling conditions in order to achieve a solid/liquid growth with a desired interfacial flux G and front velocity v_f.
Application of magnetic fields is known to stabilize both flow and temperature oscillations in the melt and thereby represents a promising opportunity to obtain an improved crystal quality. The effects of a constant magnetic field on melt convection has been previously investigated by several authors [5]-[8]. The effects of a strong vertical magnetic field on convection and segregation in the vertical Bridgeman crystal growth process was considered by Kim et al. [7], while Ben Hadid et al. [8] investigated its effect on the horizontal Bridgeman growth. A constant magnetic field suppresses thermo-solutal flow, but the inter-dendritic flows and macro-segregation patterns are not significantly affected by the magnetic field. Grants et al. [9] used a rotating magnetic field (RMF) in the growth of GaAs. The RMF was shown to affect the heat flux and the interface curvature. But there are some drawbacks to the application of a uniform magnetic field to influence growth. Any significant convection damping requires prohibitively large magnetic fields. The magnetic field must be oriented in a specific direction relative to the bulk flow for the Lorentz force to take effect and most significantly, the technique cannot be used for electrically non-conducting materials. In [10], the authors have investigated the effect of magnetic gradients on the quality of the crystal. A magnetic gradient superimposed on a uniform magnetic field caused substantial reduction in convection and resulted in a much better crystal. In the present work, the effect of a (time varying) combined magnetic field and magnetic gradient on the control of melt flow is investigated. The extension of the methodology presented here to other conducting and non-conducting materials is provided in [11]-[12].
The sequencing of the various sections of the present work is as follows. The physics of the problem of interest is presented along with the governing equations. The inverse solidification problem is then posed as a functional optimization problem. An example illustrating the formulation is provided next. Finally, some conclusions and possible extension of the work presented here are discussed.

GOVERNING EQUATIONS OF THE DIRECT PROBLEM

Let Ω be a closed bounded region with a piece-wise smooth boundary Γ. The region is filled with an incompressible, nonconducting fluid. At time $t = 0$, a part of the boundary is cooled below the freezing temperature of the fluid. When the temperature drops below the freezing temperature, solidification begins along that boundary. Let us denote the solid region by Ω_s (boundary defined by $\Gamma_{s1} \bigcup \Gamma_{s2}$) and the liquid region by Ω_l (boundary defined by Γ_l). These regions share a common solid-liquid interface boundary Γ_I.
The governing equations for the binary alloy solidification system are now introduced. Let, L be the characteristic length of the domain; ρ, the density; k, the thermal conductivity; α ($\alpha \equiv k/\rho c$), the thermal diffusivity; D, the solute diffusivity and ν, the kinematic viscosity of the liquid melt. For clarity of the analysis, and furthermore, to understand the effect of competing complex processes, the system is analyzed in a non-dimensionalized form. The characteristic scale for time is taken as L^2/α and for velocity as α/L. The dimensionless temperature is defined as $\theta \equiv (\hat{T} - T_o)/\Delta T$, where $\hat{T}$, T_o and ΔT are the temperature, reference temperature and reference temperature drop, respectively. Similarly, the dimensionless concentration is given as $c \equiv (\hat{c} - c_o)/\Delta c$, where $\hat{c}$, c_o and Δc are the concentration, reference concentration and reference concentration drop, respectively.
The motion of a fluid element in the melt is due to the various forces acting on it. In the context of the present work, there are two main body forces acting on the fluid element, namely the solutal and thermally-induced buoyancy forces. These two forces can be written as:

$$\mathbf{f}_{buoyancy} = \rho_o g \beta_T (T - T_o) \mathrm{e}_g + \rho_o g \beta_C (c - c_o) \mathrm{e}_g \tag{1}$$

where e_g is the unit vector in the direction of the gravity and the rest of the notation is standard. The non-dimensional form of this force involves the use of the thermal and solutal Rayleigh numbers. An externally applied magnetic field acts on the whole domain Ω. The externally applied magnetic field affects both the energy and the momentum of the system. These effects include the so-called

phenomenological cross-effects which can be placed into the following general categories: galvomagnetic, thermomagnetic and thermoelectric effects [13]. With the classical MHD assumptions of non-relativistic flow and quasi-magnetostatics, the electro-magnetic force on the system becomes:

$$\mathbf{f} = \mathbf{J} \times \mathbf{B} + \nabla \mathbf{B} \cdot \mathbf{M} \tag{2}$$

where, $\mathbf{M}$ is the magnetization, $\mathbf{M} = \frac{\chi_m}{\mu_m(1+\chi_m)}\mathbf{B}$, μ_m the permeability of free space and χ_m the magnetic susceptibility. The assumption of a non-conducting fluid reduces this force to the Kelvin force:

$$\mathbf{f_{Kelvin}} = \nabla \mathbf{B} \cdot \mathbf{M} \simeq \frac{\chi_m}{2\mu_m} \nabla B^2 \tag{3}$$

This provides the ability to exert a magnetizing force depending on the magnitude of the magnetic susceptibility. According to the Curie-Weiss law, the mass magnetic susceptibility χ of a paramagnetic material is inversely proportional to its absolute temperature. The above equation can be rewritten by replacing the magnetic susceptibility, χ_m with the mass magnetic susceptibility, χ, in the following way:

$$\mathbf{f_{Kelvin}} = \frac{\rho\chi}{2\mu_m} \nabla B^2 \tag{4}$$

Most materials found in nature are diamagnetic. For a diamagnetic fluid, the mass susceptibility is independent of temperature, but the magnetizing force appears due to the change in density in the above equation. Toshio et al. [14] have derived a Boussinesq approximation for this force term:

$$\mathbf{f_{Kelvin}} = \frac{\beta\chi\rho_o}{2\mu_m}(T - T_0)\nabla B^2 = \frac{\rho_o\beta\chi}{\mu_m}(T - T_0)\mathbf{B} \cdot \nabla \mathbf{B} = \frac{\chi \mathbf{B} \cdot \nabla \mathbf{B}}{\mu_m g}\rho_o g\beta(T - T_0) = \gamma\rho_o g\beta(T - T_0) \tag{5}$$

where $\gamma \equiv \frac{\chi B_i \frac{\partial B_j}{\partial x_i}}{\mu_m g}$. Notice the similarity of the form of the force terms in Eqs. (1) and (5). The form of the body force in Eq. (5) can be considered to be the product of two terms; the magnetic field $\mathbf{B}$, and the magnetic gradient,$\nabla\mathbf{B}$. Thus, $\mathbf{f_{Kelvin}}$ can be controlled independently in different ways, for example, by varying the direction and/or magnitude of the magnetic field $(B_x(t), B_y(t), B_z(t))$ or, by varying the magnitude of each of the components of the gradient tensor. Magnetic Resonance Imaging (MRI) machines can be used to simultaneously apply controlled magnetic fields and magnetic field gradients. Use of such magnetic fields is important for reliable imaging of human tissue [15]. Rapid progress in MRI imaging has resulted in the commercial production of linear magnetic fields producing gradient coils [16].

In the context of control using magnetic fields, it is possible to control the Kelvin force term in at least six independent ways. But in the present work, the variation in the Kelvin force is assumed to be only due to changes in the magnetic field. That is, the magnetic gradients are kept fixed and any variation in the Kelvin force is due corresponding changes to the magnetic field $\mathbf{B}(t)$. Further, since the aim of using magnetic field is to control the convection causing forces, the magnetic field is oriented in the direction of buoyancy, i.e. $\mathbf{B} = B\mathrm{e}_g$.

The basic equations that govern the evolution of the solidifying system are given in BOX I. They are given in terms of the following dimensionless groups: Prandtl number, $(Pr \equiv \nu/\alpha)$, Lewis number $(Le \equiv \alpha/D)$, thermal Rayleigh number $(Ra_T \equiv g\beta_T\Delta T L^3/\nu\alpha)$ and solutal Rayleigh number $(Ra_c \equiv g\beta_c\Delta c L^3/\nu\alpha)$. In addition, $R_k \equiv k_s/k_l$ is the ratio of the thermal conductivities of the solid and liquid, $Ste \equiv (C_p\Delta T)/L_H$ is the Stefan number, κ is the partition coefficient and $\delta \equiv c_o/\Delta c$ is the ratio of the reference concentration c_o and reference concentration drop Δc. In the above definitions, C_p is the heat capacity of the liquid melt, L_H is the latent heat of solidification, g is the gravity constant, β_T is the thermal coefficient of expansion and β_c is the solutal coefficient of expansion.

THE INVERSE MELT FLOW CONTROL PROBLEM

The design objective is to produce a growth that is purely diffusion-dominated thus leading to a better quality of the crystal. The design definition for the problem can be stated as follows:

'Find the time history of the externally applied magnetic field such that the solidification process defined by the equations in BOX I proceeds with negligible convection over the whole time domain.'
The design definition implies that the convection causing buoyancy force has to be neutralized by the Kelvin force. The thermal/solutal buoyant force is either parallel or anti-parallel to the gravity vector. As mentioned earlier, the magnetic gradient is assumed to be non-zero only in the direction of gravity. It follows that, γ is proportional to $B\frac{dB}{dz}$. The applied field is non-dimensionalized with the initial field B_o, and the non-dimensionalized field is referred to as $b(t)$ $(= \frac{B(t)}{B_o})$. The Kelvin force is therefore represented as $\gamma_0 b Ra_T \theta \mathbf{e}_g$, where γ_0 is $\frac{\chi B_o \frac{dB}{dz}}{\mu g}$. The design definition can now be restated as follows:
'Given the IBVP defined by the equations in BOX I and the magnitude of the superimposed magnetic gradient, $\frac{dB}{dz}$, find the time history of the imposed uniform magnetic field, $b(t)$, so that melt convection is minimized.'
To achieve a diffusion-based growth the magnetic field must be chosen in such a way so as to negate the effects of the thermal and solutal buoyancy. The objective is restated in terms of $b(t) \in L_2[0, t_{max}]$. We are looking for an optimal solution $\bar{b}(t) \in L_2[0, t_{max}]$ such that:

$$S(\bar{b}) \leq S(b) \qquad \forall\ b \in L_2[0, t_{max}] \tag{6}$$

where

$$S(b) = \frac{1}{2} \| \mathbf{v}(\mathbf{x}, t; b) \|^2_{L_2(\Omega \times [0, t_{max}])} = \frac{1}{2} \int_0^{t_{max}} \int_\Omega \mathbf{v}(\mathbf{x}, t; b) \cdot \mathbf{v}(\mathbf{x}, t; b) d\Omega dt \tag{7}$$

In the above equation, $\mathbf{v}(\mathbf{x}, t; b)$ is defined as the melt flow for the direct solidification problem with an applied field corresponding to b and a given superimposed magnetic gradient $\frac{dB}{dz}$. The domain used to define the cost functional can be considered as Ω or Ω_l since the velocity $\mathbf{v} = 0$ in the solid phase. The main difficulty with the above optimization problem is the calculation of the gradient $S'(b(t))$ of the cost functional in the $L_2(\Omega \times [0, t_{max}])$ space. Introducing the directional derivative $D_{\Delta b} \equiv (S'(b), \Delta b)_{L_2(\Omega \times [0, t_{max}])}$ of $S(b)$, and using the definition of the cost functional, we can write the following.

$$D_{\Delta b} S(b) \equiv (S'(b), \Delta b)_{L_2(\Omega \times [0, t_{max}])} = (\mathbf{v}(\mathbf{x}, t; b), \mathbf{V}(\mathbf{x}, t; b, \Delta b))_{L_2(\Omega \times [0, t_{max}])} \tag{8}$$

where the sensitivity velocity field $\mathbf{V}(\mathbf{x}, t; b, \Delta b) \equiv D_{\Delta b} \mathbf{v}(\mathbf{x}, t; b)$ and the sensitivity temperature field and the sensitivity concentration field written as $\Theta(\mathbf{x}, t; b, \Delta b) \equiv D_{\Delta b} \theta(\mathbf{x}, t; b)$ and $C(\mathbf{x}, t; b, \Delta b) \equiv D_{\Delta b} c(\mathbf{x}, t; b)$, respectively are defined as the linear Δb parts of $\theta(\mathbf{x}, t; b)$, $\mathbf{v}(\mathbf{x}, t; b)$ and $c(\mathbf{x}, t; b)$ calculated at b.

$$\theta(\mathbf{x}, t; b + \Delta b) = \theta(\mathbf{x}, t; b) + \Theta(\mathbf{x}, t; b, \Delta b) + O(\| \Delta b \|^2_{L_2(\Omega \times [0, t_{max}])}) \tag{9}$$

$$\mathbf{v}(\mathbf{x}, t; b + \Delta b) = \mathbf{v}(\mathbf{x}, t; b) + \mathbf{V}(\mathbf{x}, t; b, \Delta b) + O(\| \Delta b \|^2_{L_2(\Omega \times [0, t_{max}])}) \tag{10}$$

$$c(\mathbf{x}, t; b + \Delta b) = c(\mathbf{x}, t; b) + C(\mathbf{x}, t; b, \Delta b) + O(\| \Delta b \|^2_{L_2(\Omega \times [0, t_{max}])}) \tag{11}$$

As is clear from Eq. (8), the calculation of the gradient $S'(b)$ requires the evaluation of the adjoint to the sensitivity of the velocity operator.
Taking the directional derivatives of the governing equations of BOX I in the direction of Δb and calculated at the direct fields $\theta(\mathbf{x}, t; b)$, $c(\mathbf{x}, t; b)$ and $\mathbf{v}(\mathbf{x}, t; b)$ corresponding to the imposed field b results in a linear sensitivity solidification problem that can be used to evaluate the fields $\Theta(\mathbf{x}, t; b)$, $C(\mathbf{x}, t; b)$ and $\mathbf{V}(\mathbf{x}, t; b)$. This sensitivity problem is summarized in BOX II, where $\Sigma(\mathbf{x}, t; b, \Delta b)$ and $\Pi(\mathbf{x}, t; b, \Delta b)$ are used to denote the directional derivatives of the stress $\sigma(\mathbf{x}, t; b)$ and pressure $p(\mathbf{x}, t; b)$, respectively.
The calculation of the gradient of the objective function requires the appropriate evaluation of the adjoint operators to the sensitivity operators. The adjoint temperature is represented as ψ. ω and ρ represent the adjoint velocity and adjoint concentration, respectively. The derivations of the adjoint equations are given in [11]-[12]. The finally obtained sensitivity and adjoint systems of equations are given below in BOX II and BOX III, respectively.

BOX I Direct problem

Solve for $\mathbf{v}(\mathbf{x},t;b)$, $\theta(\mathbf{x},t;b)$ and $c(\mathbf{x},t;b)$

- Melt region

$$\nabla\cdot\mathbf{v}(\mathbf{x},t)=0,\quad (\mathbf{x},t)\in\Omega_l(t)\times[0,t_{max}]$$

$$\frac{\partial\mathbf{v}(\mathbf{x},t)}{\partial t}+\mathbf{v}(\mathbf{x},t)\cdot\nabla\mathbf{v}(\mathbf{x},t)=-\nabla p+Pr\nabla^2\mathbf{v}(\mathbf{x},t)+Ra_TPr\theta_l(\mathbf{x},t)\mathbf{e}_g$$
$$-Ra_cPrc(\mathbf{x},t)\mathbf{e}_g-Ra_TPr\gamma_0b\theta_l(\mathbf{x},t)\mathbf{e}_g,\quad (\mathbf{x},t)\in\Omega_l(t)\times[0,t_{max}]$$

$$\frac{\partial c(\mathbf{x},t)}{\partial t}+\mathbf{v}(\mathbf{x},t)\cdot\nabla c(\mathbf{x},t)=Le^{-1}\nabla^2c(\mathbf{x},t),\quad (\mathbf{x},t)\in\Omega_l(t)\times[0,t_{max}]$$

$$\frac{\partial\theta_l(\mathbf{x},t)}{\partial t}+\mathbf{v}(\mathbf{x},t)\cdot\nabla\theta_l(\mathbf{x},t)=\nabla^2\theta_l(\mathbf{x},t),\quad (\mathbf{x},t)\in\Omega_l(t)\times[0,t_{max}]$$

$$\frac{\partial\theta_l(\mathbf{x},t)}{\partial n}=0,\quad \frac{\partial c(\mathbf{x},t)}{\partial n}=0,\quad (\mathbf{x},t)\in\Gamma_l(t)\times[0,t_{max}]$$
$$\mathbf{v}(\mathbf{x},t)=0,\quad (\mathbf{x},t)\in\Gamma_l(t)\times[0,t_{max}]$$
$$\mathbf{v}(\mathbf{x},0)=0,\ c(\mathbf{x},0)=c_i,\ \theta(\mathbf{x},0)=\theta_i,\quad \mathbf{x}\in\Omega_l(t=0)$$

- Solid zone

$$\frac{\partial\theta_s(\mathbf{x},t)}{\partial t}+\mathbf{v}(\mathbf{x},t)\cdot\nabla\theta_s(\mathbf{x},t)=\nabla^2\theta_s(\mathbf{x},t),\quad (\mathbf{x},t)\in\Omega_s(t)\times[0,t_{max}]$$

$$\theta_s(\mathbf{x},0)=\theta_i,\quad \mathbf{x}\in\Omega_s(t=0)$$

$$\frac{\partial\theta_s(\mathbf{x},t)}{\partial n}=0,\ (\mathbf{x},t)\in\Gamma_{s1}\times[0,t_{max}],\theta_s(\mathbf{x},t)=\theta_{s2},(\mathbf{x},t)\in\Gamma_{s2}\times[0,t_{max}]$$

- Interface

$$R_k\frac{\partial\theta_s(\mathbf{x},t)}{\partial t}-\frac{\partial\theta_l(\mathbf{x},t)}{\partial t}=Ste^{-1}\mathbf{V_f}\cdot\mathbf{n},\quad (\mathbf{x},t)\in\Gamma_I(t)\times[0,t_{max}]$$

$$\theta(\mathbf{x},t)=\theta_0+mc(\mathbf{x},t),\quad (\mathbf{x},t)\in\Gamma_I(t)\times[0,t_{max}]$$

$$\frac{\partial c(\mathbf{x},t)}{\partial n}=Le(k-1)(c(x,t)+\delta)\mathbf{V_f}\cdot\mathbf{n},\quad (\mathbf{x},t)\in\Gamma_I(t)\times[0,t_{max}]$$

Using the definition of the adjoint operators defined above the following relations are obtained:

$$D_{\Delta b}S(b)\equiv(S'(b),\Delta b)_{L_2(\Omega_l\times[0,t_{max}])}=(\mathbf{v},\mathbf{V})_{L_2(\Omega_l\times[0,t_{max}])}$$
$$(\omega,Ra_tPr\Delta b\gamma_0\theta\mathbf{e}_g)=(\mathbf{V},Ra_TPr\mathbf{v})\qquad(12)$$

BOX II Sensitivity problem

Solve for $\mathbf{V}(\mathbf{x},t;b,\Delta b)$, $\Theta(\mathbf{x},t;b,\Delta b)$ and $C(\mathbf{x},t;b,\Delta b)$

- Melt region

$$\nabla\cdot\mathbf{V}(\mathbf{x},t)=0,\quad (\mathbf{x},t)\in\Omega_l(t)\times[0,t_{max}]$$

$$\frac{\partial\mathbf{V}(\mathbf{x},t)}{\partial t}+\mathbf{V}(\mathbf{x},t)\cdot\nabla\mathbf{v}(x,t)+\mathbf{v}(x,t)\cdot\nabla\mathbf{V}(\mathbf{x},t)=-\nabla\Sigma-Ra_cPrC(x,t)\mathbf{e}_g$$
$$+Ra_TPr(1-\gamma_0 b)\Theta(\mathbf{x},t)\mathbf{e}_g-Ra_TPr\Delta b\gamma_0\theta(x,t)\mathbf{e}_g,\quad (\mathbf{x},t)\in\Omega_l(t)\times[0,t_{max}]$$

$$\mathbf{\Sigma}(\mathbf{x},t)=-\Pi(\mathbf{x},t)\mathbf{I}+Pr[\nabla\mathbf{V}(\mathbf{x},t)+(\nabla\mathbf{V}(\mathbf{x},t))^T],\quad (\mathbf{x},t)\in\Omega_l(t)\times[0,t_{max}]$$

$$\frac{\partial C(\mathbf{x},t)}{\partial t}+\mathbf{v}(\mathbf{x},t)\cdot\nabla C(\mathbf{x},t)+\mathbf{V}(\mathbf{x},t)\cdot\nabla c(\mathbf{x},t)=Le^{-1}\nabla^2C(\mathbf{x},t),$$
$$(\mathbf{x},t)\in\Omega_l(t)\times[0,t_{max}]$$

$$\frac{\partial\Theta(\mathbf{x},t)}{\partial t}+\mathbf{v}(\mathbf{x},t)\cdot\nabla\Theta(x,t)+\mathbf{V}(\mathbf{x},t)\cdot\nabla\theta(\mathbf{x},t)=\nabla^2\Theta(\mathbf{x},t),$$
$$(\mathbf{x},t)\in\Omega_l(t)\times[0,t_{max}]$$

$$\frac{\partial\Theta(\mathbf{x},t)}{\partial n}=0,\frac{\partial C(\mathbf{x},t)}{\partial n}=0,\quad (x,t)\in\Gamma_l(t)\times[0,t_{max}]$$

$$\mathbf{V}(\mathbf{x},t)=0,\quad (\mathbf{x},t)\in\Gamma_l(t)\times[0,t_{max}]$$

$$\mathbf{V}(\mathbf{x},0)=0,C(\mathbf{x},0)=0,\Theta(\mathbf{x},0)=0,\quad \mathbf{x}\in\Omega_l(t=0)$$

- Interface

$$R_k\frac{\partial\Theta_s(\mathbf{x},t)}{\partial n}-\frac{\partial\Theta_l(\mathbf{x},t)}{\partial n}=Ste^{-1}\tilde{\mathbf{V}}_f\cdot\mathbf{n},\quad (\mathbf{x},t)\in\Gamma_I(t)\times[0,t_{max}]$$

$$\Theta(\mathbf{x},t)=mC(\mathbf{x},t),\quad (\mathbf{x},t)\in\Gamma_I(t)\times[0,t_{max}]$$

$$\frac{\partial C(\mathbf{x},t)}{\partial n}=Le(k-1)(c(\mathbf{x},t)+\delta)\tilde{\mathbf{V}}_f\cdot\mathbf{n}+Le(k-1)C(\mathbf{x},t)\mathbf{V}_f\cdot\mathbf{n},$$
$$(\mathbf{x},t)\in\Gamma_I(t)\times[0,t_{max}]$$

The gradient of the cost function can therefore be written in terms of the adjoint variables

$$S'(b)\equiv\gamma_0\theta(\omega\cdot\mathbf{e}_g)\tag{13}$$

Once the gradient of the cost functional is found, any gradient-based optimization method can be used to solve the optimization problem. In the present work the conjugate gradient method is used.

BOX III Adjoint problem

Solve for $\omega(\mathbf{x},t;b,\Delta b)$, $\psi(\mathbf{x},t;b,\Delta b)$ and $\rho(\mathbf{x},t;b,\Delta b)$

$$-\frac{\partial \omega}{\partial t} - \mathbf{v}\cdot\nabla\omega + \omega\cdot\nabla\mathbf{v}^T + \nabla\pi - Pr\nabla^2\omega - Ra_T Pr\psi\nabla\theta + Ra_c Pr\rho\nabla c + Ra_T Pr\mathbf{v} = 0, \quad (\mathbf{x},t)\in\Omega_l(t)\times[0,t_{max}]$$

$$-\frac{\partial \rho}{\partial t} - u\cdot\nabla\rho - Le^{-1}\nabla^2\rho + \omega\cdot\mathbf{e}_g = 0, \quad (\mathbf{x},t)\in\Omega_l(t)\times[0,t_{max}]$$

$$-\frac{\partial \psi}{\partial t} - u\cdot\nabla\psi - \nabla^2\psi + (1-\gamma_0 b)\omega\cdot\mathbf{e}_g = 0, \quad (\mathbf{x},t)\in\Omega_l(t)\times[0,t_{max}]$$

$$\frac{\partial\psi(\mathbf{x},t)}{\partial n} = 0, \frac{\partial\rho(\mathbf{x},t)}{\partial n} = 0, \quad (\mathbf{x},t)\in(\Gamma_l(t)-\Gamma_I(t))\times[0,t_{max}]$$

$$\omega(\mathbf{x},t) = 0, \quad (\mathbf{x},t)\in\Gamma_I(t)\times[0,t_{max}]$$

$$\Theta\frac{\partial\psi}{\partial n} = \psi(\frac{\partial\Theta}{\partial n}), \quad (\mathbf{x},t)\in\Gamma_I\times[0,t_{max}]$$

$$C\frac{\partial\rho}{\partial n} = \rho(\frac{\partial C}{\partial n}), \quad (\mathbf{x},t)\in\Gamma_I\times[0,t_{max}]$$

$$\omega(\mathbf{x},t_{max}) = 0,\ \rho(\mathbf{x},t_{max}) = 0,\ \psi(\mathbf{x},t_{max}) = 0, \quad \mathbf{x}\in\Omega_l(t=0)$$

NUMERICAL EXAMPLE

In this section, solidification of a salt solution in a rectangular cavity is considered. The physical properties of the system are taken as $Pr = 6.44$, $Ra_T = 200000$, $Ra_C = 10000$, $Le = 1000$ and $Ste = 0.034$. The initial temperature of the melt is $1C$. The right wall is maintained at $-10C$ for the duration of the simulation. The other walls are thermally insulated (see [17] for more details on the problem setup). The freezing temperature of the fluid is $-10C$. The growth was simulated for a dimensionless time of 0.1. The melt computational domain consisted of 1200 quadrilateral elements and 1271 nodes, while the solid computational domain consisted of 800 quadrilateral elements and 861 nodes. The inverse design problem examined here is the following:
'Find the magnetic field $b(t)$ such that convection-less solidification growth leading to a vertical freezing interface is achieved during the process defined by the problem of Box I'.
The time domain $[0,\tau_{max}]$ is taken with $\tau_{max} = 0.1$. This is chosen, because beyond this time the temperature of the melt reaches a temperature close to the freezing temperature and the velocity in the melt region is negligible. An initial guess of $b^0(t) = 1$ is used to start the CGM iterations. Within each CGM iteration, the direct, adjoint and sensitivity problems are solved using a deforming finite element method. The spatial and temporal discretization remain the same for all three problems. The total number of time steps involved in the solution of each of the direct, sensitivity and adjoint problems is 201. The total computational time for each CGM iteration including the solution of the three subproblems was about 2.5 hours on a Pentium 4 processor. This included considerable time spent on reading/writing data as the adjoint and the sensitivity problems require the direct problem

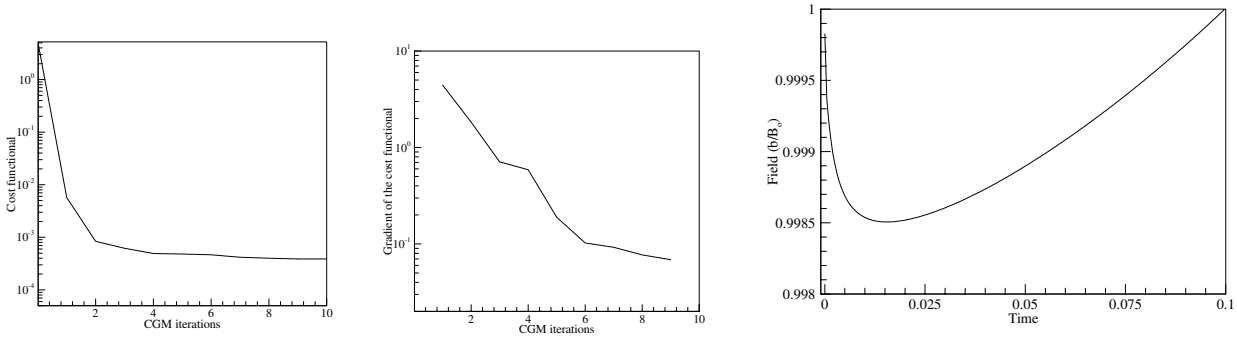

Figure 1: (a) Cost functional, (b) Gradient of the cost functional and (c) Converged optimal field.

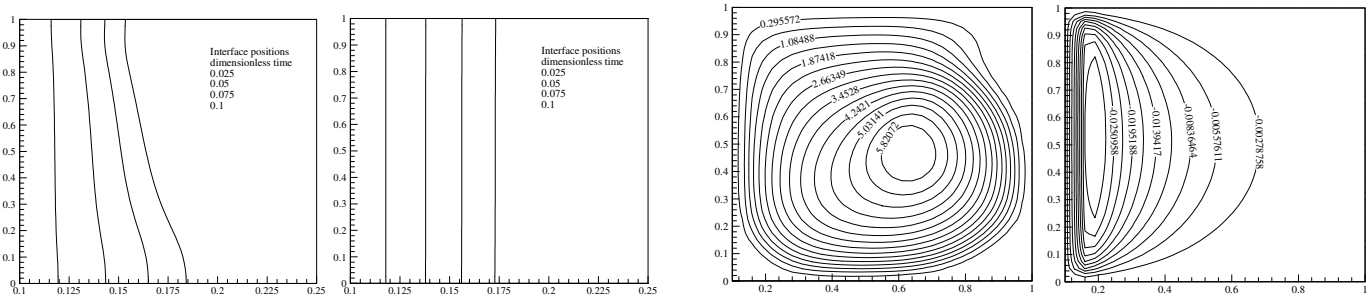

Reference case Optimal case Reference case Optimal case

Figure 2: Comparison of the interface positions and streamline contours.

solution at each time step of their solution. The convergence of the CGM is shown in Fig. 1(a). The computations were stopped after the cost functional reached a specified error tolerance of 5×10^{-4}. The gradient of the cost functional which determines the approach to the optimal solution is plotted against the iteration counter in Fig. 1(b).

The temporal variation of the optimal external magnetic field to be applied is given in Fig. 1 (c). At very early times the buoyant force is purely due to the thermal gradients present as a result of the lower temperature at the left wall. The magnetic gradient is at the maximum value of $b = 1.0$ during this time. When solidification starts at the left wall, there is immediately solute rejection into the melt from the solidified material. This changes the solute concentration along the interface non-uniformly. This non-uniformity in concentration coupled with the movement of the heavier solute towards the bottom of the cavity leads to a concentration gradient. The concentration gradient, in turn, leads to a solutal buoyant force that acts in the direction opposite to the thermal buoyant force. To make the net body force zero, the optimization algorithm compensates for the decreased body force by correspondingly decreasing the magnetic field such that the sum of the three body forces cancel each other out. With increasing time, since a diffusion-based growth is attained, the solute is rejected all along the interface in to the melt. This leads to a uniform distribution of concentration along the interface. Hence, the solutal buoyant force gradually reduces. This reduction in the solutal buoyant force is in turn compensated by an increase in the magnetic field at later times. In order to see how close the desired objectives were met a comparison of the optimal solution with a reference case was made. The reference case involved running the direct problem for no applied magnetic case while the optimal solution involved running the direct problem with the magnetic gradient obtained from the converged CGM optimization scheme.

To evaluate whether the desired flat interface is obtained, the interface positions and shapes for the reference case and the optimal case are shown in Fig. 2. The optimal magnetic gradient ensures a perfectly planar growth front. To evaluate weather the desired convection-less growth is achieved,

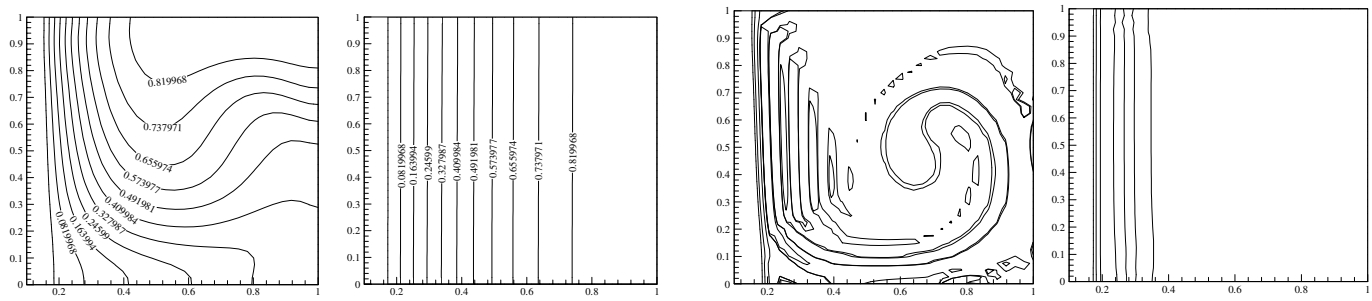

Reference case Optimal case Reference case Optimal case

Figure 3: Comparison of isotherms and isochors.

isotherms of the reference case as well as the optimal solution are plotted in Fig. 3. Under the action of the optimal magnetic gradient the isotherms are parallel to the moving front at all times during the growth simulation. The substantial suppression of velocity in the melt is brought out by the streamline contours shown in Fig. 2. The maximum strength of the vorticity reduced from $\omega_{max} = 5.82$ to about $\omega_{max} = 0.025$. As a consequence of a planar interface and diffusion dominated growth, the concentration evolution is also diffusion-based. A comparison of the isochors of the two above mentioned cases is provided in Fig. 3. Compare the uniform distribution of the solute along the length of the interface under the action of the magnetic gradient to the isochors for the reference case. The solute is uniformly distributed along the length of the interface. This results in a homogeneous distribution of the solute in the solid.

CONCLUSIONS

A systematic continuum formulation using the adjoint method was proposed for the design of the solidification process. The objective was the control of the externally applied magnetic field such that the solidification of the material proceeds in a convection-less environment. An inverse design problem was defined and the exact gradient of the cost functional was obtained using the solution of an adjoint system of equations. The non-linear conjugate gradient method was used to solve for the optimal magnetic field. The application of the optimal calculated magnetic field along with a superimposed magnetic gradient resulted in the uniform growth of the interface and suppression of temperature and concentration fluctuations in the solid. It has been shown that, through proper application of a magnetic field and magnetic field gradient(s), a state of earth-based reduced gravity growth, resulting in better quality of crystals can be achieved.

The present methodology can be further extended to the design of the orientation as well as the magnitude of the magnetic field along with the thermal fluxes (furnace design) to include broader design conditions. With the demonstrated potential of the developed methodology to the solidification of non-conducting materials, we are currently investigating using magnetic field gradients in the controlled crystallization of proteins. Applications to the solidification and crystal growth of conducting materials can be found in Reference [12].

ACKNOWLEDGEMENTS

The work presented here was funded by the NASA Microgravity Materials Science Program (grant NAG8-1671). This research was conducted using the resources of the Cornell Theory Center, which receives funding from Cornell University, New York State, federal agencies, and corporate partners.

References

[1] A.N. Tichonov, Solutions of Ill-Posed Problems, *Halsted Press, New York* (1977)

[2] M.D. Gunzburger, H.C. Lee, *Analysis, approximation, and computation of the coupled solid/fluid temperature control problem*, Comp. Meth. App. Mech. Engn. 118, (1994), 133-152

[3] G.Z. Yang, N. Zabaras, *The adjoint method for an inverse design problem in the directional solidification of binary alloys*, J. Comp. Phys. 140, (1998), 432-452

[4] R. Sampath, N. Zabaras, *Adjoint variable method for the thermal design of eutectic directional solidification processes in an open-boat configuration*, Num. Heat Transfer:Part A, 39, (2001), 655-683

[5] G.M. Oreper, J. Szekely, *The effect of a magnetic field on transport phenomena in a Bridgeman-Stockbarger crystal growth*, J. Crys. Growth, 67, (1984), 405-421

[6] S. Motakef, *Magnetic field elimination of convective interference with segregation during vertical Bridgmenn growth of doped semi-conductors*, J. Crys. Growth, 64, (1990), 550-560

[7] D.H. Kim, P.M. Adoranto, R.A. Brown, *Effect of vertical magnetic field on convection and segregation in vertical Bridgeman growth*, J. Crys. Growth, 89, (1988), 339-350

[8] H. Ben Hadid and B. Roux, *Numerical study of convection in the horizontal Bridgeman configuration under the action of a constant magnetic field. 1. Two dimensional flow*, J. Fluid Mech, 333, (1997), 23-37

[9] O. Patzold, I. Grants, U. Wunderwald, K. Jenker, A. Croll, G. Gerbeth, *Vertical gradient freeze growth of GaAs with a rotating nagnetic field*, J. Crys. Growth, 245, (2002), 237-246

[10] B. Ganapathysubramanian, N. Zabaras, *Using magnetic field gradients to control the directional solidification of alloys and the growth of single crystals*, J. Crys. Growth, submitted for publication

[11] B. Ganapathysubramanian, N. Zabaras, *Advanced control of solidification using tailored magnetic fields. Part I - Non-conducting materials*, J. Crys. Growth, submitted for publication

[12] B. Ganapathysubramanian, N. Zabaras, *Advanced control of solidification using tailored magnetic fields. Part II - Conducting materials*, J. Crys. Growth, submitted for publication

[13] G. Dulikravich, *Unified Electro-Magneto-Fluid Dynamics (EMFD)- A survey of mathematical models*, Int. J. Non Linear Mech. 32(5), (1997), 923-932

[14] T.Tagawa, R. Shigemitsu, H. Ozoe, *Magnetizing force modelled and numerically solved for natural convection of air in a cubic enclosure: effect of the direction of the magnetic field*, Int. J. Heat Mass Transfer 45, (2002), 267-277

[15] J.P. Hornak, *The Basics Of MRI*, http://www.cis.rit.edu/htbooks/mri/

[16] S.R. Thomas, L.J. Busse, J.F. Schenck, *Gradient Coil Technology*, In Magnetic Resonance Imaging, ed. by C.L. Partain, R.R. Price, J.A. Patton, M.V. Kulkarni, A.E. James Saunders, Philadelphia (1988)

[17] J. W. Evans, C. D. Seybert, F. Leslie, W. K. Jones, *Supression/reversal of natural convection by exploiting the temperature/composition dependance of magnetic susceptibility*, J. App. Phys. 88(7), (2000), 4347-4351